Preparation and Characterization of Microcellular Polystyrene Foams Processed in Supercritical Carbon Dioxide

Kelyn A. Arora, Alan J. Lesser,* and Thomas J. McCarthy*

Polymer Science and Engineering Department, University of Massachusetts, Amherst, Massachusetts 01003

Received December 11, 1997; Revised Manuscript Received May 4, 1998

ABSTRACT: The foaming of polystyrene using supercritical (SC) CO_2 has been studied to better understand the microcellular foaming process, as we plan future studies that involve the creation of composite microcellular foams. Rapid decompression of SC CO_2-saturated polystyrene at sufficiently high temperatures (above the depressed T_g) yields expanded microcellular foams. The resulting foam structures can be controlled by manipulating processing conditions. Experiments varying the foaming temperature while holding other variables constant show that higher temperatures produce larger cells and reduced densities. Structures range from isotropic cells in samples retaining their initial geometry to highly expanded foams recovered in the shape of the foaming vessel and having oriented, anisotropic cells and limited density reduction. Higher saturation pressures lead to higher nucleation densities and hence smaller cells. Decreasing the rate of depressurization permits a longer period of cell growth and therefore larger cell sizes. Foams having a bimodal distribution of cell sizes can be created by reducing the pressure in two stages.

Introduction

We have reported a novel method for producing polymer composite materials that involves the supercritical fluid (SCF)—assisted infusion of vinyl monomers into, and subsequent free-radical polymerization within, organic polymer substrates.[1,2] Styrene can be polymerized within semicrystalline and amorphous polymer substrates to create polymer blends with kinetically trapped morphologies. We have recently begun to use this approach to create composite microcellular foams using SC CO_2 as the solvent for chemical modification reactions and as the foaming agent.

Others have demonstrated that CO_2 can be used to foam amorphous materials such as poly(methyl methacrylate), polystyrene, polycarbonate, and poly(ethylene terephthalate).[3−9] Typically, a polymer sample is saturated with CO_2 (or nitrogen) at room temperature and subsequently removed from the vessel and foamed by heating to a temperature above the normal glass transition (T_g) in a high-temperature bath. Goel and Beckman[3,4] have reported a different foaming method in which the polymer is saturated with CO_2 at relatively high temperatures and pressures (in the supercritical (SC) regime) followed by rapid depressurization to atmospheric pressure at constant temperature. This method takes advantage of the depression of T_g by CO_2. CO_2 is known to swell and significantly plasticize many amorphous polymers, often reducing the glass transition to temperatures approaching room temperature.[10−14]

SCFs offer many desirable properties as both solvents and foaming agents including adjustable solvent strength,[15−17] plasticization, and enhanced diffusion rates.[16,17] Since CO_2 is a gas at ambient conditions, the solvent rapidly dissipates upon release of pressure. A pressure quench from SCF conditions at constant temperature also ensures that no vapor/liquid boundary is encountered which can damage the cellular structure of a foam. Finally, CO_2 presents an obvious environmental advantage over conventional CFC (chlorofluorocarbon) foaming agents or organic solvents.

We report here the preparation of microcellular polystyrene using SC CO_2 as a foaming agent in a method similar to that described by Goel and Beckman.[3,4] The initial targets for foamed polymer blends consist of a matrix polymer and an incipient polystyrene phase. The experiments described here were envisioned as single-component control experiments for the blend expansion studies. We found the single-component studies, however, to be quite rich on their own. The cellular structure resulting from this type of foaming procedure can be readily controlled by manipulating such processing parameters as temperature, pressure, depressurization profile, and vessel size. Isotropic foams with uniform cell size can be prepared as well as foams with oriented, anisotropic cells and foams with bimodal distributions of cell sizes.

Experimental Section

Materials. Polystyrene was purchased from Scientific Polymer Products in the form of pellets and used as received or compression molded at 150 °C into $^1/_{16}$-in.-thick plaques. The molecular weight was measured using a Polymer Laboratories gel permeation chromatograph with THF as the mobile phase and found to be $M_n = 67\,000$ with a polydispersity of 2.3. The reported density was 1.04 g/cm^3, and infrared spectroscopy showed no measurable impurities. CO_2 (Coleman Grade, 99.99%) was purchased from Merriam Graves and used as received.

Foam Preparation. Foams were prepared in 316 stainless steel hexagonal high-pressure vessels (10-mL volume) containing glass culture tubes as liners to facilitate removal of the foamed samples. Polystyrene, in the form of pellets or a compression-molded plaque, was weighed and placed in the glass tube inside the steel vessel. The vessel was preheated and filled with SC CO_2 to the desired pressure using a heated high-pressure CO_2 manifold.[1] It was then placed in a circulating oil bath to soak at the foaming temperature for a prescribed period of time until saturation conditions were reached. At the end of this period, the vessel was depressurized at the soak temperature following one of two protocols. For rapid depressurization to atmospheric conditions, a valve was opened, immediately venting the CO_2. For depressurization over a

S0024-9297(97)01811-1 CCC: $15.00

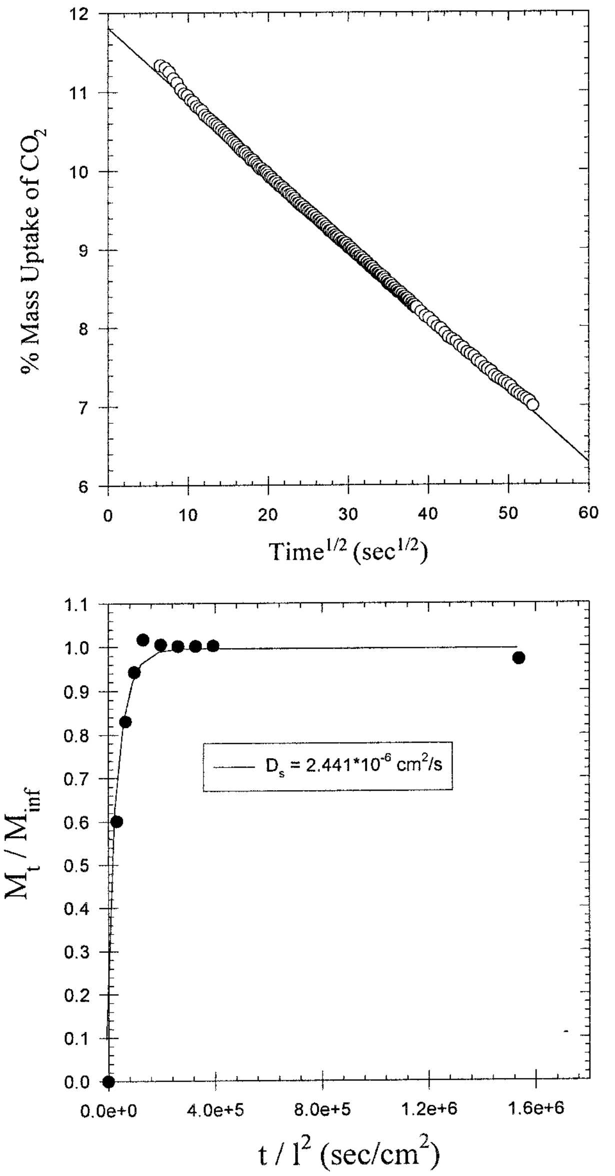

Figure 1. Absorption of CO_2 into polystyrene at conditions of 80 °C and 3530 psi. The upper plot shows a representative (6-h absorption) desorption profile. An equilibrium mass uptake of 11.8% CO_2 is attained in 2−3 h. The lower plot indicates the kinetics for absorption showing mass absorbed divided by equilibrium mass absorbed for absorption times of 1−22 h. The diffusivity during absorption was calculated to be 2.44×10^{-6} cm^2/s.

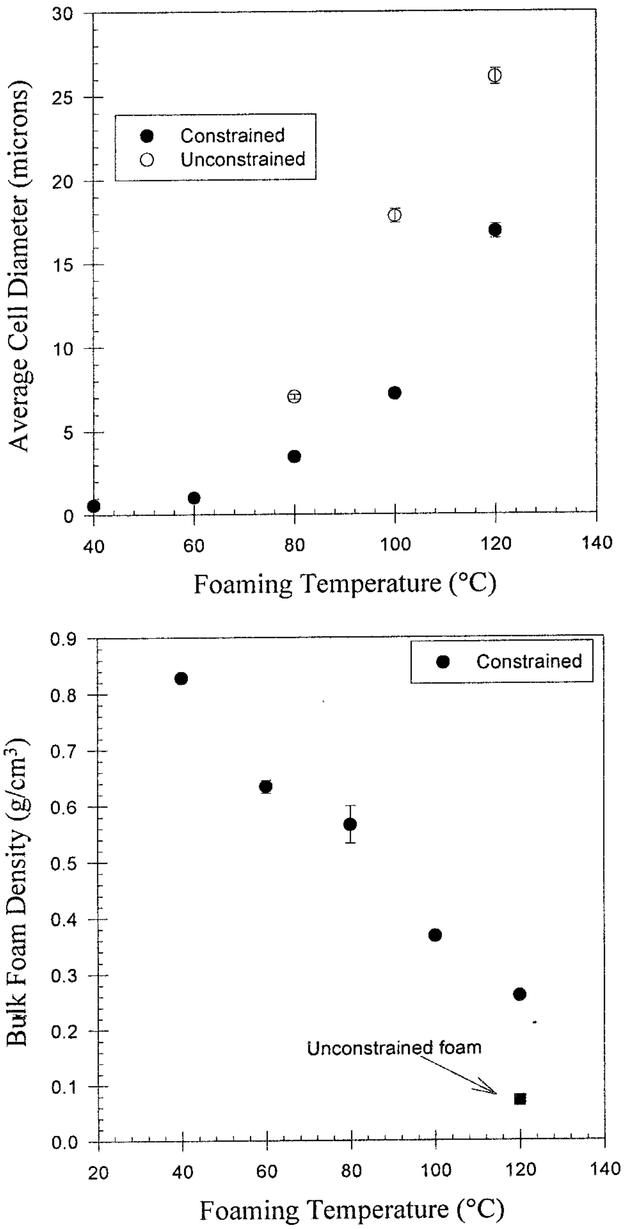

Figure 2. Effects of foaming temperature on the average cell size and bulk foam density of polystyrene foams. Saturation pressure was kept constant at 3530 psi, and depressurization was rapid.

period of time or release of the pressure to an intermediate pressure, a back pressure regulator was connected and used to control the pressure drop. After decompression, the vessel was removed from the temperature bath and allowed to cool, and the specimen was removed.

Foam Characterization. The foams were characterized to determine their densities, cell sizes, and cell shapes. Densities were calculated by measuring the volume of water displaced by the sample and dividing this value into the sample mass. Three measurements were taken and averaged for each sample, and the standard error was calculated. There was no obvious uptake of water by the samples during the measurement process, which, if it occurred, would bias the density measurements.

The cellular structure was examined by cryofracturing the specimen at liquid N_2 temperature, sputter-coating with approximately 200 Å of gold, and viewing with a JEOL 35CF scanning electron microscope (SEM). Zeiss Image Analysis software was used to measure the average value and distribution of properties of the foam such as the cell diameter, cell wall thickness, and aspect ratio.

Results and Discussion

Absorption/Desorption Kinetics. The equilibrium solubility and kinetics for absorption and desorption of CO_2 in polystyrene (from which the CO_2 diffusivity can be calculated) at a given set of processing conditions (80 °C, 3530 psi) were measured according to the method described by Berens.[16,17] Tared $^1/_{16}$ in.-thick compression-molded polystyrene samples were placed in individual reaction vessels, which were then purged with CO_2, filled to the desired pressure and temperature, and left to soak for prescribed periods of time. After rapid venting of the vessels, the samples were removed and immediately transferred to a balance interfaced to a computer to record mass loss as a function of time. From these measurements, the percent mass uptakes were calculated and the results plotted versus the

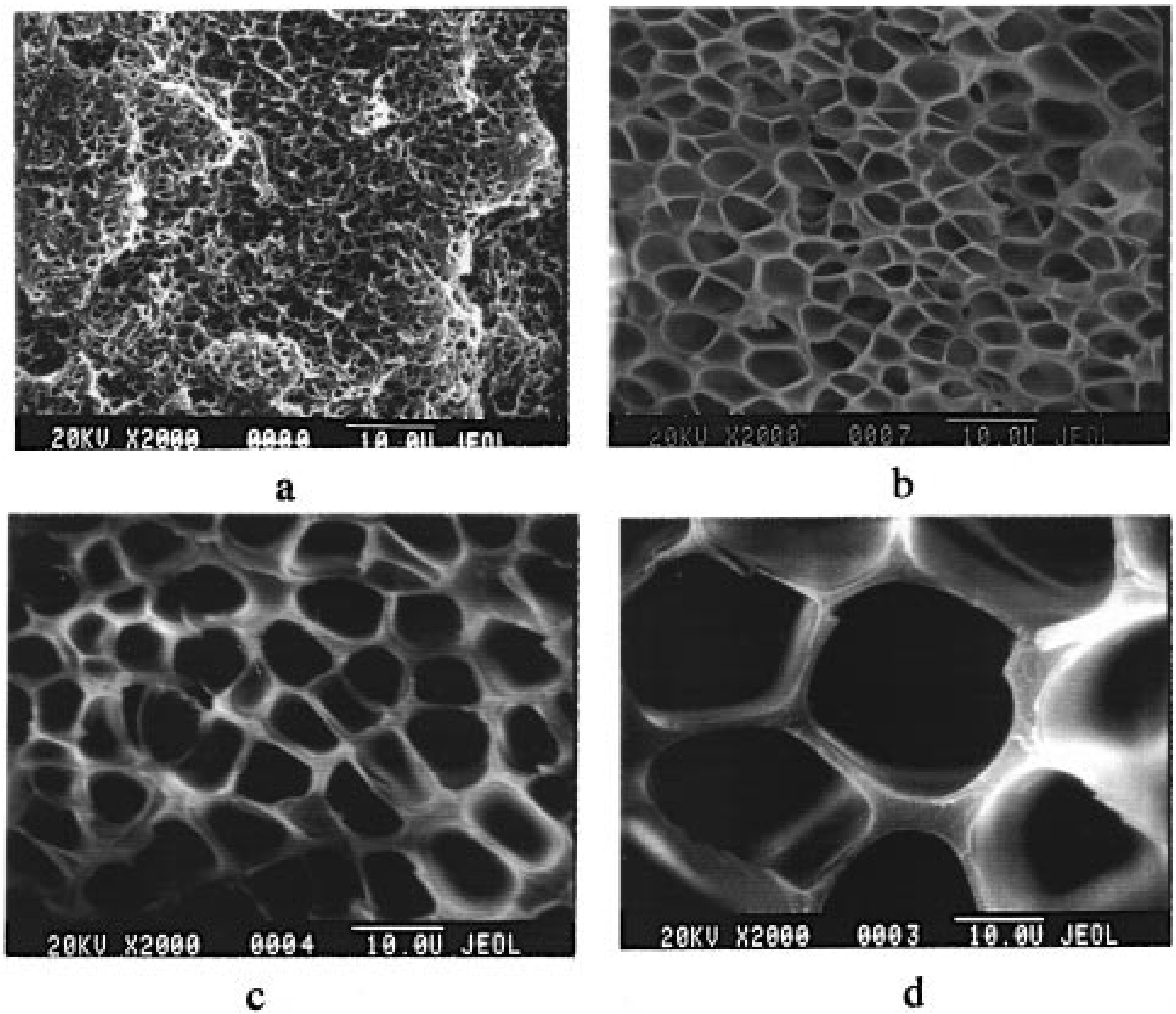

Figure 3. SEM micrographs illustrating temperature effects on the cellular structure of polystyrene foams: (a) 40 °C, (b) 80 °C, (c) 100 °C, (d) 120 °C. All foams were prepared under 3530 psi of CO_2 pressure and rapidly depressurized.

square root of desorption time. This yielded linear plots indicative of Fickian diffusion kinetics. Linear extrapolation to zero desorption time gives the uptake of CO_2 at the end of the sorption period. A series of sorption times were studied to determine when equilibrium was reached.

Figure 1 shows a representative plot (6-h absorption) for desorption of CO_2 from polystyrene. The linearity of the data indicates Fickian behavior. An equilibrium uptake of 11.8% CO_2 is absorbed within 2−3 h. It should be noted that the samples foamed upon depressurization, although they retained their planar shape for all but the longest soak times. As a result, only the *absorption* kinetics and diffusivity can be accurately measured since CO_2 is leaving the sample by diffusing through the polystyrene and by creating pores, rendering the desorption a more complex system.

The diffusivity of CO_2 into polystyrene was calculated using the equation derived by Crank[18] for diffusion in a plane sheet:

$$\frac{M_t}{M_\infty} = 1 - \sum_{n=0}^{\infty}\left[\frac{8}{(2n+1)^2\pi^2}\exp\left\{\frac{-D(2n+1)^2\pi^2}{4l^2}\right\}\right]$$

where M_t = mass uptake at time t, M_∞ = equilibrium mass uptake, D = diffusivity (cm^2/s), and l = original unfoamed thickness.

One-dimensional diffusion can be assumed since the thickness is much smaller than the other dimensions. Based on Crank's equation, a plot (also in Figure 1) was made of M_t/M_∞ vs t/l^2 and curve-fit to solve for the diffusivity which was found to be 2.44×10^{-6} cm^2/s under these conditions. This value must be regarded as an estimate, as D is a function of CO_2 concentration which changes over the course of the experiment.

Based upon this information, all soak times for temperatures at or above 80 °C were greater than 3 h to ensure maximum CO_2 uptake. Foams made at temperatures lower than 80 °C were soaked overnight.

Variables Which Control Foam Structure. (i) Temperature. Since this method of foaming relies on the depression of T_g of the substrate by supercritical CO_2 to allow for cell growth, the temperature at which the material is foamed has a profound effect on the cells produced. Increasing the temperature decreases the viscosity of the substrate material, causing the retractive force restricting cell growth to decrease and the diffusivity of CO_2 within the substrate to increase.

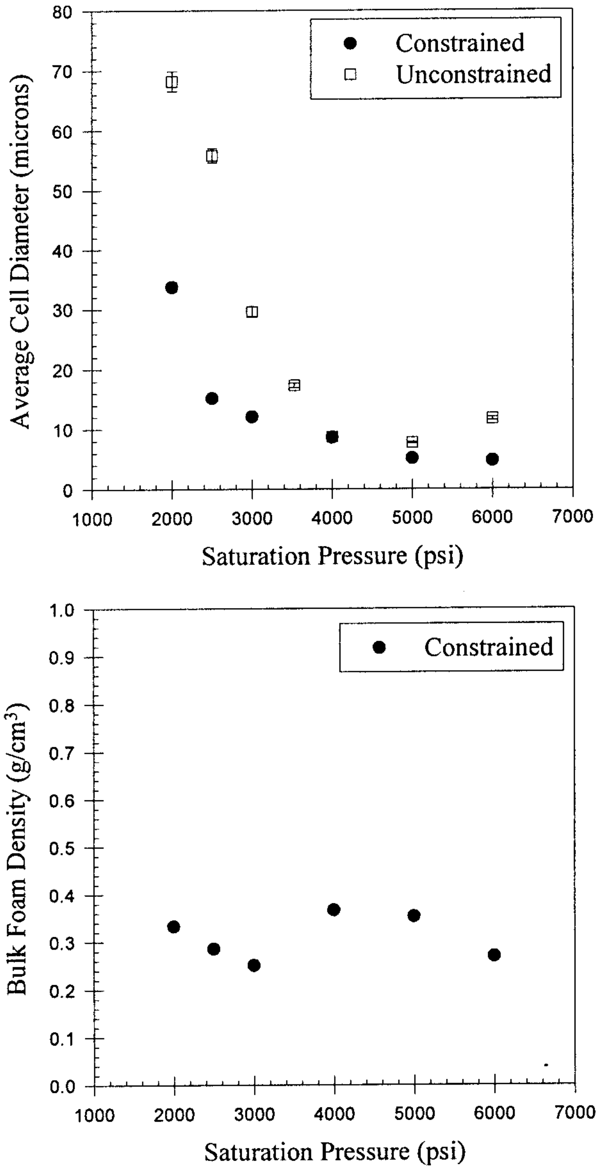

Figure 4. Effects of saturation pressure on the average cell diameter and bulk density of polystyrene foams. Foams were prepared at a constant temperature of 100 °C and rapidly depressurized.

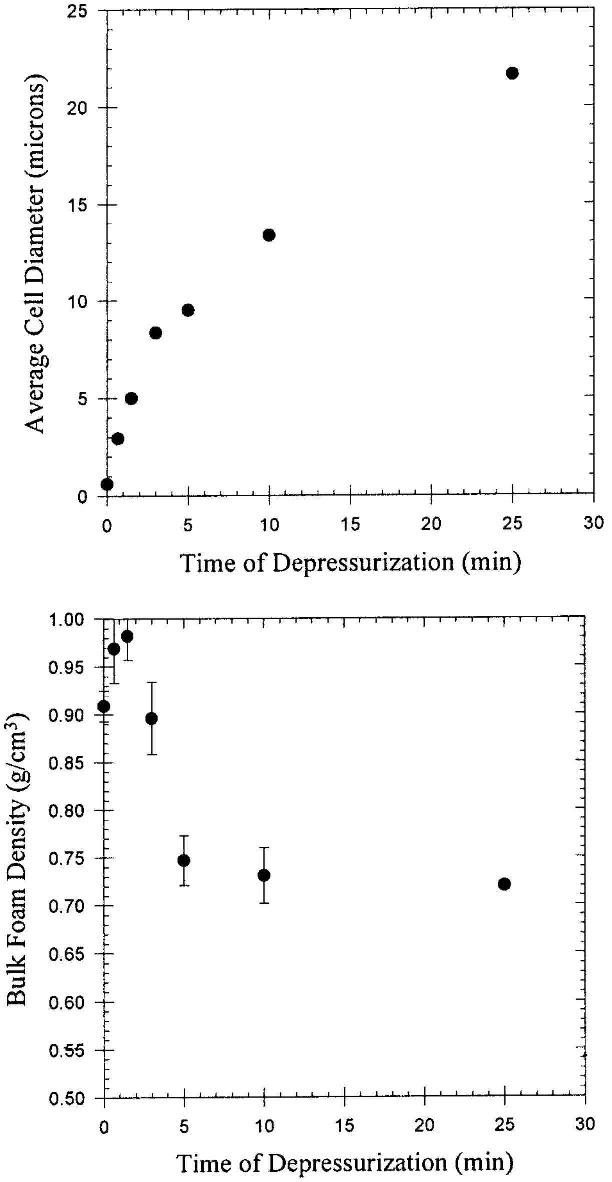

Figure 5. Effects of depressurization rate on the average cell size and bulk density of polystyrene foams. Saturation conditions were 40 °C and 3530 psi.

These factors lead to more rapid cell growth. At a constant pressure, higher temperatures require a lower CO_2 density. This leads to a lower degree of swelling by CO_2 and thus fewer nuclei generated, allowing for larger cells. In addition, at higher temperatures, less CO_2 is required to depress the T_g of polystyrene below the soak temperature. Thus, the higher the temperature, the longer the time (at a given decompression rate) cells have to grow before vitrification.

Wang et al.[10] have shown that the T_g of polystyrene is depressed by CO_2 to 30−40 °C at 200 atm of pressure. This result indicates that polystyrene should be able to be foamed at temperatures only slightly above room temperature. A series of polystyrene foams was produced at various temperatures while holding the saturation pressure (3530 psi) and depressurization time (1−2 s) constant. Figure 2 shows that the cell size increases roughly exponentially with temperature, while the density decreases linearly. Accompanying this increase in cell size is a change in the nature of the cells from discrete, spherical cells in a polystyrene matrix to a structure consisting of impinging, polygonal cells (Figure 3). The overall appearance of the foams varies from whitened planar sheets (at lower temperatures) to expanded cylindrical specimens in the shape of the foaming vessel (at higher temperatures).

For the highly expanded foams, both cell size and density reduction are limited by the size of the foaming vessel (or the amount of polystyrene placed in the vessel). To ascertain the extent of this volume constraint, a series of "unconstrained" foams were prepared by expanding single polystyrene pellets in the same size vessels. The pellets were able to expand without contacting the walls of the vessel. The data for these foams are also shown in Figure 2. As expected, these "unrestricted" foams exhibit larger cell sizes than their constrained counterparts but show the same trend with increasing temperature. These experiments indicate that the size of the foaming vessel (or the amount of material in it) is another variable which can be used to control foam density and cell size. We have also shown that gradient density/cell size foams can be prepared by using a variable diameter (tapered) vessel.

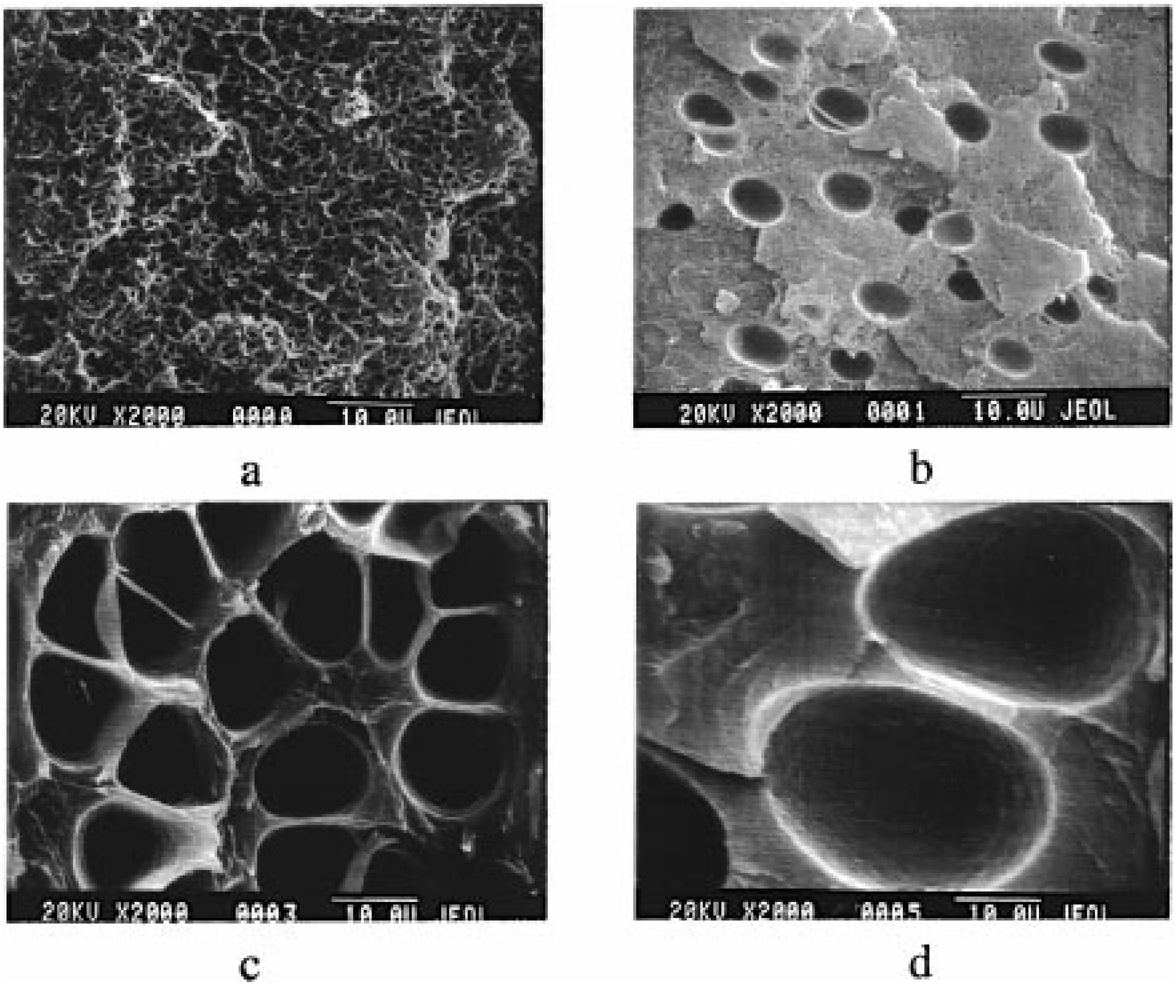

Figure 6. SEM micrographs showing the growth of cells in polystyrene foams made at 40 °C and 3530 psi with varying depressurization times: (a) 1 s, (b) 1 min, (c) 5 min, (d) 25 min.

(ii) Pressure. The effect of the saturation pressure on the foam structure was studied for decompression at a constant temperature of 100 °C. Figure 4 shows that the cell size decreases with increasing saturation pressure. At higher pressures, the amount of CO_2 incorporated into the substrate is higher, and hence the substrate is more highly supersaturated upon release of pressure. In addition, homogeneous nucleation theory[3] predicts that, as the magnitude of the pressure drop increases, the energy barrier to nucleation decreases, leading to more cells being nucleated within a given volume. This would lead to smaller cell sizes overall. Figure 4 shows that cell size does indeed decrease with increasing saturation pressure. As in the previous set of experiments, the constrained foams have smaller cells than their unconstrained counterparts. The density reduction of the constrained foams was limited to approximately 0.3 g/cm^3 due to the volume constraints of the vessel, as equal amounts of polystyrene were expanded into the same total volume.

(iii) Depressurization Rate. A series of experiments was carried out in which the rate of depressurization was varied while holding the saturation conditions constant at 40 °C and 3530 psi. These initial conditions were chosen because of the small cell sizes produced at instantaneous depressurization and the planar structure of the resulting foam. This allowed for significant cell growth to occur without the constraint of a limited foaming vessel volume. As is seen in Figure 5, when allowed time to develop, the cells are able to grow much larger (22 μm) than when depressurization is rapid (0.6 μm). Density, however, levels off at a value of ~0.72 g/cm^3. The micrographs shown in Figure 6 indicate that the cells retain their spherical geometry but grow larger in size. In order for the density of the sample to remain constant as the cell size increases (cells/volume decreases), coalescence may be occurring during the longer depressurization times.

(iv) Depressurization Profile. With the exception of the foams discussed below, all of the polystyrene foams produced have fairly uniform cell sizes with normal or log-normal size distributions. We were, however, also able to produce foams which were distinctly bimodal by modifying the foaming procedure.

To create foams with a bimodal distribution of cell sizes, the polystyrene was first soaked under conditions of high temperature and pressure until saturated and subsequently depressurized to an intermediate pressure (6000 to 4000 psi). The vessel was then maintained at this pressure for 1 h before releasing the remaining pressure. The resulting foam displays a clear bimodal structure with the small and large cells interdispersed as shown in Figure 7a,c. This bimodal structure is evident throughout the length and cross section of the foam sample. To determine which cell size was created as a result of the first decompression step, a sample saturated at 100 °C and 6000 psi was depressurized to 4000 psi, held at this pressure for 1 h, and then cooled to 0 °C in an ice/water bath (at a constant fluid density) to freeze in the intermediate microstructure before

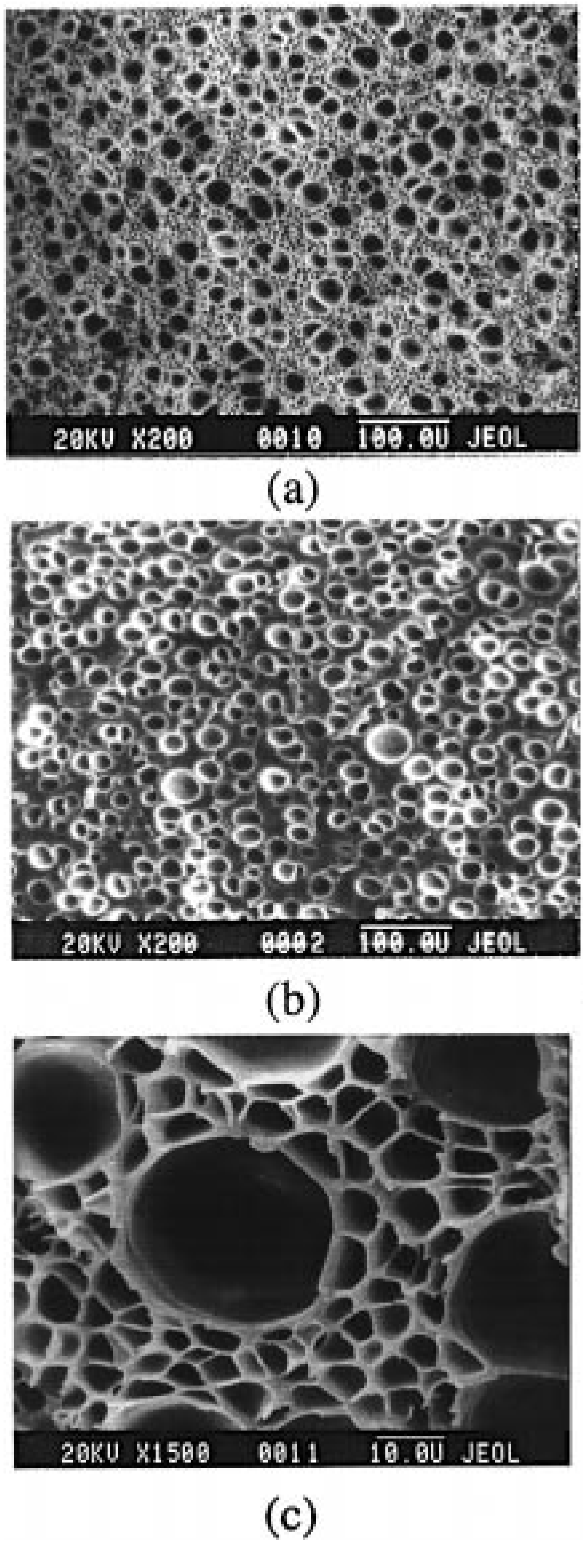

Figure 7. Examining the creation of a bimodal cellular structure in polystyrene foams. (a) 100 °C, 6000 psi, pressure was released to 4000 psi, held at this pressure for 1 h, and then released to atmospheric pressure. Average cell sizes are 21 and 4.8 μm. (b) 100 °C, 6000 psi, pressure was released to 4000 psi and held for 1 h before releasing the remaining pressure at 0 °C to capture the intermediate microstructure. Average cell size is 18 μm. (c) Sample a at a higher magnification.

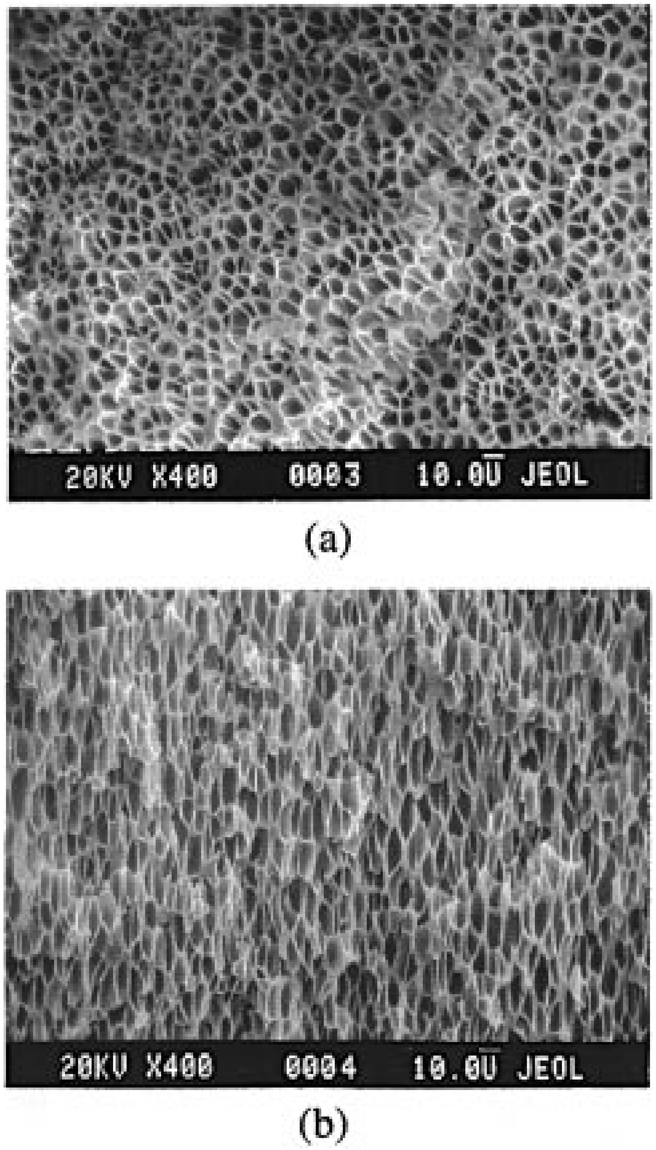

Figure 8. Micrographs of a polystyrene foam produced at 100 °C 6000 psi in a cylindrically shaped vessel. (a) Viewed perpendicular to the cylinder axis. (b) Viewed parallel to the cylinder axis.

releasing the remaining pressure. A comparative analysis of this microcellular structure and that of a foam that underwent the entire staged decompression indicates that phase separation takes place between 6000 and 4000 psi. The phase separation leads to the formation of spherical domains of SCF CO_2, which, in turn, leads to the formation of the larger cells. During the second depressurization stage, a second set of cells is nucleated and grown within the walls of this first set. The resulting structures are shown in Figure 7.

(v) Vessel Geometry. The highly expanded foam samples described above were prepared in cylindrically shaped glass liners. The cell sizes reported were measured by fracturing the samples across the diameter of the cylinder and viewing the cross section. Examination of this cross section reveals isotropically impinging, polygonal cells. When the foam is fractured parallel to the cylinder axis, however, it is evident that the cells are elongated along the length of the cylindrical shape. During the expansion process the foam is confined radially by the walls of the glass liner and further expansion is restricted to the direction parallel to the cylinder axis. The cells are thus drawn into elliptical geometries (see Figure 8). This elongation is not observed in foams that retain their initial geometries

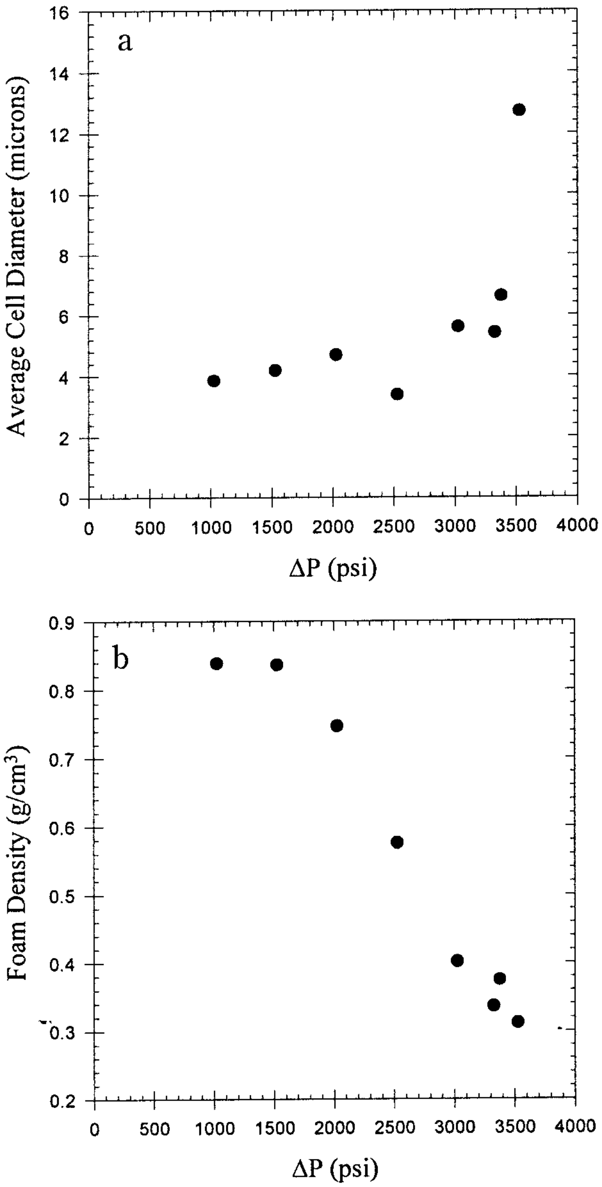

Figure 9. Studying the growth of cells in polystyrene foams from 100 °C and 3530 psi. The system was cooled to 0 °C after partial release of pressure to trap the resulting intermediate microstructure. (a) Effect of pressure drop on the average cell diameter. (b) Effect of pressure drop on bulk foam density.

(planar sheet). The anisotropy is also more pronounced as the magnitude of the pressure drop increases.

(vi) Depth of Pressure Quench. A series of experiments was carried out in which the polystyrene was soaked in CO_2 at 100 °C and 3530 psi of CO_2 until saturated, and then the pressure was released to various intermediate pressures between 3530 psi and atmospheric pressure. The vessel was then cooled to 0 °C in an ice/water bath (at a constant fluid density), preventing further cell growth before releasing the remaining pressure. The driving force for cell growth in these foams is the supersaturated condition of the polystyrene after the external pressure is released. The amount by which the pressure is dropped controls the degree of supersaturation and thus has an effect on cell size and structure. This series of experiments was designed to provide "snapshots" indicating how the cells grow as the pressure is decreased to atmospheric pressure. Significant growth of the cells does not occur until the CO_2 pressure is below the critical point (P_c = 1070 psi, $\Delta P \sim$ 2500 psi), where it is more compressible (see Figure 9). The densities of the foams remain fairly constant until they drop off sharply at a pressure slightly higher than the critical pressure. As the cells grow larger, they also change from discrete, spherical cells to impinging, polygonal cells.

Summary

The foaming of polystyrene using SC CO_2 as the blowing agent has been studied in detail. An equilibrium mass uptake of 11.8% CO_2 is absorbed by polystyrene at conditions of 80 °C, 3530 psi. The structure of the foams produced can be tailored by altering the various processing conditions. A higher foaming temperature produces foams with larger cells and lower densities. Higher saturation pressures increase the nucleation density, leading to smaller cells. The size of the vessel in which the material is foamed can restrict its growth and hence affects cell sizes, cell shapes, and foam densities. Reducing the rate of depressurization allows for a longer period of growth and therefore larger cells than with rapid decompression. Bimodal foams have been produced by reducing the pressure in stages, and oriented, anisotropic foams are produced when the polystyrene becomes highly expanded.

Acknowledgment. We thank the NSF-sponsored Materials Research Science and Engineering Center and the Office of Naval Research for financial support. K.A.A. acknowledges support from the National Science Foundation in the form of a Graduate Research Fellowship.

References and Notes

(1) Watkins, J. J.; McCarthy, T. J. *Macromolecules* **1994**, *27*, 4845.
(2) Watkins, J. J.; McCarthy, T. J. *Macromolecules* **1995**, *28*, 4067.
(3) Goel, S. K.; Beckman, E. J. *Polym. Eng. Sci.* **1994**, *34*, 1137.
(4) Goel, S. K.; Beckman, E. J. *Polym. Eng. Sci.* **1994**, *34*, 1148.
(5) Kumar, V.; Weller, J. E. *ANTEC* **1991**, 1401.
(6) Kumar, V.; Van Der Wel, M. M. *ANTEC* **1991**, 1406.
(7) Kweeder, J. A.; Ramesh, N. S.; Campbell, G. A.; Rasmussen, D. H. *ANTEC* **1991**, 1398.
(8) Baldwin, D. F.; Park, C. B.; Suh, N. P. *Polym. Eng. Sci.* **1996**, *36*, 1437.
(9) Baldwin, D. F.; Park, C. B.; Suh, N. P. *Polym. Eng. Sci.* **1996**, *36*, 1446.
(10) Wang, W.-C. V.; Kramer, E. J.; Sachse, W. H. *J. Polym. Sci., Polym. Phys. Ed.* **1982**, *20*, 1371.
(11) Condo, P. D.; Johnston, K. P. *J. Polym. Sci., Part B: Polym. Phys.* **1994**, *32*, 523.
(12) Chiou, J. S.; Barlow, J. W.; Paul, D. R. *J. Appl. Polym. Sci.* **1985**, *30*, 2633.
(13) Goel, S. K.; Beckman, E. J. *Polymer* **1993**, *34*, 1410.
(14) Baldwin, D. F.; Gustafson, D. E.; Suh, N. P.; Shimbo, M. *ANTEC* **1993**, 1840.
(15) Wissinger, R. G.; Paulaitis, M. E. *J. Polym. Sci., Part B: Polym. Phys.* **1987**, *25*, 2497.
(16) Berens, A. R.; Huvard, G. S. *Supercrit. Fluid Sci. Technol.* **1989**, 208.
(17) Berens, A. R.; Huvard, G. S.; Korsmeyer, R. W.; Kunig, F. W. *J. Appl. Polym. Sci.* **1992**, *46*, 231.
(18) Crank, J. *The Mathematics of Diffusion*, 2nd ed.; Clarendon Press: Oxford, 1975.

MA971811Z